Journal of Environmental Chemical Engineering 3 (2015) 1794–1801

Contents lists available at ScienceDirect

Journal of Environmental Chemical Engineering

journal homepage: www.elsevier.com/locate/jece

Removal of iron–cyanide complexes from wastewaters by combined UV–ozone and modified zeolite treatment

Sergio Hanela[a,b,*], Jorge Durán[a], Silvia Jacobo[b]

[a] Programa de Tecnologías de Tratamiento (PTT), Centro de Tecnología del Uso del Agua (CTUA), Instituto Nacional del Agua (INA), Au. Ezeiza-Cañuelas km.1.62 (1804), Buenos Aires, Argentina
[b] Departamento de Química, Facultad de Ingeniería, Universidad de Buenos Aires (UBA) – INTECIN -Av. Paseo Colón 850 (1063), Buenos Aires, Argentina

ARTICLE INFO

Article history:
Received 27 January 2015
Accepted 22 June 2015
Available online 26 June 2015

Keywords:
Cyanide
Iron
Complex
Advanced oxidation
Uv–ozone
Wastewater treatment

ABSTRACT

A treatment system was developed to remove iron-complexed cyanide from wastewaters discharged by small surface finishing workshops. Alkaline chlorination, a widely used treatment method, does not remove iron–cyanide complexes and produces chlorine secondary pollution effects. In this work, the effectiveness of a bench scale system with a UV–ozone step, followed by a fixed bed made of manganese-modified natural zeolite was studied to remove potassium hexacyanoferrate(II) $K_4[Fe(CN)_6]$. The system was operated on a semi-continuous basis processing up to 7.2 l batches of synthetic wastewater. The optimal residence time was established by feeding the system with a free iron solution and using a residence time distribution (RTD) model.

With the employed experimental conditions, a 66% cyanide removal was observed at the UV–ozone stage. The fixed bed retained 55% of the total iron fed and an additional 5% of iron was precipitated. Cyanide removal was slightly increased by fixed bed up to 68%. This method achieved a significant removal of iron–cyanide complexes. The results were analysed by using an RTD model and a mechanism for the processes occurred was proposed. Technical and economical scaling up conditions must be studied in future works to assess the feasibility of treating wastewaters from small electroplating workshops.

Introduction

Numerous industrial activities such as mining, electroplating, steel tempering, nylon production and others use cyanide in their operations [1–3]. Other processes like coking and gasification of coal, blast furnace operation, alumina reduction and municipal sludge incineration generate cyanide as an undesirable by-product [1]. Therefore, cyanide compounds are usually found in wastewaters from those industries [1–4]. When cyanide comes into contact with dissolved metal ions, metal–cyanide complexes are formed. Depending on the metal involved, these complexes may be weak acid dissociable (WAD) as is the case of Ag, Cd, Cu, Ni, Zn, Hg or strong acid dissociable (SAD) such as Fe, Au, Co, Pt or Pd complexes. Some of the above-mentioned industrial processes, as is the case of electroplating, involve iron-based materials in contact with cyanide solutions. For that reason, iron-cyanide complexes are also found in wastewaters from such industries [2,4,5].

Due to the high toxicity of cyanide, its total concentration in effluents released to the environment is stringently regulated worldwide. Uncomplexed cyanide, also called free cyanide, is the most toxic form of cyanide in aqueous solutions because it is released as gaseous hydrogen cyanide when the solution pH decreases below 9.2. The toxicity of WAD complexes is also important because they dissociate by releasing the free cyanide at pH values between 4.5 and 6 [1,6]. For some time, it was held that SAD complexes were harmless because they are innocuous and require strong acidity conditions ($pH < 2$) to release free cyanide. However, low pH values may accidentally occur when industrial effluents mix in the urban sewage.

In addition to the pH effects, several authors agree on the risk of dissociation of iron-cyanide complexes when they are exposed to UV radiation [4,7–9] or even to diffuse sunlight [4,6]. This phenomenon was first observed by Ohno [10] and Shirom and Stein [11] some 40 years ago, but it was only in the last decades that it began to be associated with the potential hazards of those compounds. Nowadays, several environmental regulations restrict

Abbreviations: RTD, residence time distribution; WAD, weak acid Dissociable; SAD, strong acid dissociable; ICP, inductively coupled plasma; XRD, X-ray diffraction; ISE, ion selective electrode.

* Corresponding author: Fax: +54 11 4480 4500x2236.
E-mail addresses: shanela@ina.gob.ar (S. Hanela), jduran@ina.gob.ar (J. Durán), sjacobo@fi.uba.ar (S. Jacobo).

http://dx.doi.org/10.1016/j.jece.2015.06.023
2213-3437/

the total cyanide concentration in the wastewaters, either it was complexed or not.

There are several treatment technologies for cyanide-containing wastewaters. Some separate the cyanide in solid form (adsorption, precipitation) while others concentrate it (ion exchange, distillation, reverse osmosis). However, oxidation is the only mechanism available to destroy such a dangerous compound. The oxidation of cyanide may be chemical or biological. Cyanide oxidation by alkaline chlorination is the most widely applied technology in small and medium electroplating workshops, especially in developing countries. Though existing oxidation methods are commonly effective to treat free or weakly-complexed cyanide, they do not destroy strongly-complexed cyanide [1,2,4,9,12].

The advanced oxidation processes (AOPs) are emerging as an alternative for the treatment of wastewaters with compounds that cannot be easily oxidized by traditional methods [13–17]. AOPs includes several treatment techniques based on the in-situ generation of strong oxidant hydroxyl radicals ($OH^{\bullet}$) [18]. Those radicals increase the thermodynamic feasibility and kinetics of the oxidation reactions, are not highly selective and may attack most of the organic compounds [19]. This kind of systems involved complex reaction pathways, including several other radical species [18].

Some authors [4,20,21] analysed the possibility of removing the iron–cyanide complexes present in aqueous solutions using the $OH^{\bullet}$ radicals generated by heterogeneous photo-catalysis with titanium oxide (TiO_2) catalysts. The disadvantages of this method are mainly associated with the cost of catalyst separation from the treated water, recovery [20,22] and removal efficiency [4].

When ozone is combined with UV light, it produces strong oxidant hydroxyl radicals ($OH^{\bullet}$) and consequently this kind of system was also classified by several authors as an AOP technique [5,18,19]. The generation of hydroxyl radicals by UV–ozone systems is enhanced in alkaline aqueous media [1,23] and the kinetics of cyanide oxidation by ozone has been found to be improved by this fact [9,23]. However, iron-complexed cyanide cannot be easily oxidized by ozone or by $OH^{\bullet}$ radicals [1,9]. The UV light used in the UV–ozone reactor (253.7 nm) is capable of dissociating iron–cyanide complexes [4,5,10,11,24,25]. Once dissociated by UV, the released free cyanide may be readily oxidized by the ozone and the $OH^{\bullet}$ radicals. If the released cyanide is not completely oxidized, the remaining fraction may be quickly recombined with the iron released from the iron–cyanide complex dissociation. This recombination would seriously hinder oxidation of cyanide and should be avoided through rapid free iron removal.

To scale-up this technology for industrial applications, it will probably be necessary to recirculate part of the treated liquid to regulate operating conditions [25]. In this case, the treated liquid must be partially mixed with the raw liquid. If the treated liquid still contains uncomplexed iron and if the raw liquid still contains free cyanide, the iron will complex the cyanide and render it difficult to be treated. It is always preferable to treat free cyanide instead of its iron-complexed forms. Consequently, iron removal is very important to ensure the applicability of this technology.

Mudliar et al. [22] reported the effectiveness of the UV–ozone method in destroying metal–cyanide complexes in real wastewaters from the automobile industry using batch experiments. The samples examined by Mudliar et al. contained iron but also several other metals and compounds. The authors only reported the analysis of cyanide in treated liquid but did not analyse the behaviour of iron and other metals.

In a previous work, Wada et al. [5] presented a 4-step system to remove iron–cyanide complexes from wastewaters: (1) UV radiation with low ozone doses (1 mg/min), (2) fixed-bed adsorption of iron, (3) UV radiation with high ozone doses (9 mg/min), and (4) ion exchange (anionic and cationic). Wada et al. reported that the iron–cyanide complex was dissociated by UV radiation in step 1. The released iron was then retained in a fixed bed made of synthetic zeolite covered with manganese oxides (step 2). The cyanide that was previously dissociated from iron was then oxidized into cyanate (CNO^-) with high ozone doses (step 3). Ion exchange (step 4) finally decomposed CNO^- into CO_2 and NH_4^+ by hydrolysis, retaining NH_4^+ and reducing the treated liquid conductivity.

The aim of this paper is to modify the above-mentioned system so that it can be used for wastewater treatment in small local electroplating workshops. In this regard, it is proposed to replace the synthetic zeolite used as catalyst support with a natural zeolite extracted from a quarry in the Province of San Juan (Argentina). This material is more than 1500 times cheaper than synthetic zeolite [25] and does not have to be imported from other countries. It is also proposed to combine steps 1 and 2 into one with a single UV–ozone reactor capable of dissociating cyanide and of oxidizing it in a tandem reaction system.

Materials and methods

Synthetic wastewater characteristics (inlet solutions)

Analytical grade reagents (Merck, J.T. Baker, Anedra) and deionized water (conductivity $< 8.5\ \mu S/cm$) were used. Two different inlet solutions were employed: (a) with soluble iron(II) and (b) with soluble hexacyanoferrate(II). For (a) experiments, iron (II) sulphate ($FeSO_4{\cdot}7H_2O$) was dissolved to reach a concentration of 1.9 mg Fe/l. The solution pH was adjusted to 12.7 ± 0.1 with 12 N sodium hydroxide (NaOH) taking in account the solubility of Fe $(OH)_2$ at different pH values presented by Blesa et al. [26]. For (b) experiments, potassium hexacyanoferrate(II) ($K_4[Fe(CN)_6]{\cdot}3H_2O$) was dissolved in an alkaline solution (4 g NaOH/l) to ensure an alkaline medium. The solution was prepared with a concentration of 13.11 mg $K_4[Fe(CN)_6]$/l and the pH was 13.5 ± 0.1 pH. The authors decided not to acidify the solution up to 12.7 to prevent any possible release of gaseous hydrogen cyanide due to very low pH caused by local acidification. The solution volume varied from 20 to 40 l depending on the experiment.

Experimental system set-up

The experimental system consisted of two series-connected reactors (Fig. 1).

The solution was first pumped through a UV–ozone reactor; then it was conveyed to a fixed bed column and the treated liquid was discharged from the outlet.

The UV–ozone photo reactor (Fig. 2) was made of borosilicate glass. The reactor consisted of an open top, cylindrical tank with a low pressure mercury UV-lamp (Pura Inc., 41Y4; 16,000 W/cm^2, 11.4 UV–Watts, main emission line at 253.7 nm) concentrically suspended from the top. A fritted glass diffuser was placed at the bottom of the reactor to allow the continuous injection of ozonised gas. Ozone was produced from pure oxygen (99.5%) with an ozone

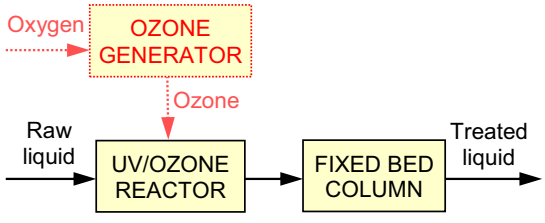

Fig. 1. Schematic diagram of the employed experimental set-up.

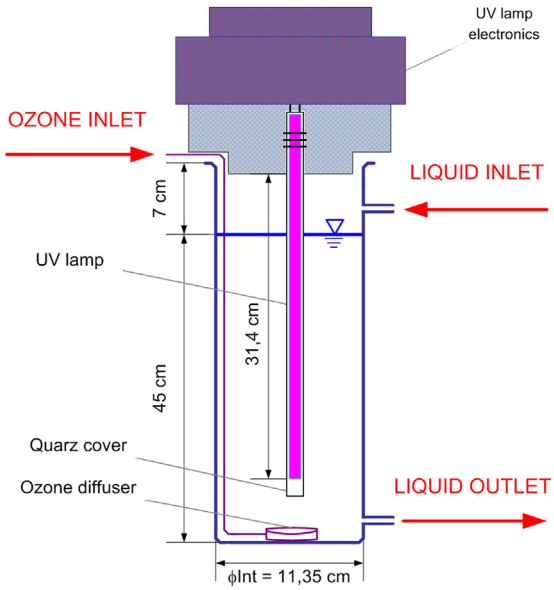

Fig. 2. Constructive detail of the UV–ozone reactor employed in the experiments.

generator (Ozonogen U.S.pat. # 4,383,976); the ozone mass flow rate (3 mg/min) was adjusted by regulating the feed voltage of the ozone generator and verified by iodometric analysis [25]. The ozonised gas flow was 1.2 ± 0.1 l/min. The liquid volume in the reactor was 4.325 l and different liquid flow rates were used for the various assays.

The fixed bed column consisted of an acrylic cylinder with a liquid inlet at the bottom. The liquid was discharged by overflow into a lateral outlet near the top (Fig. 3). Bed porosity (V_{holes}/V_{total}) was estimated at 0.4 and the liquid volume was 296 ml.

The fixed bed column was filled with natural zeolite pretreated with manganese oxides. The pretreatment method was adapted from [5]. Each batch was prepared using 1 l of raw natural zeolite (mesh 2–4 mm) stirred for 3 h in 2.5 l solution with 33.8 g $MnSO_4{\cdot}H_2O$/l. After the supernatant was decanted, the zeolite was mixed for 2 h at 97 °C with a $KMnO_4$ solution (47.4 g $KMnO_4$/l), the material was dried overnight at room temperature and then heated to 210 °C for 2 h. The resulting material was rinsed several times with reagent water until no manganese measured by ICP (<0.016 mg Mn/l) was detected in the rinsing water.

Analytical methods

The main parameters analysed during the experiments were iron (total and soluble) and cyanide (total, soluble, total free and soluble free). For soluble iron and cyanide measurements the samples were filtered immediately after collection to prevent any possible re-dissolution of solids. Filtration of samples was performed using a 0.45 μm cellulose acetate filter membrane as indicated in [6,27] for soluble iron determination. Results have an analytical accuracy of 0.05 mg/l for iron and 0.1 mg/l for cyanide determinations.

Iron concentration was determined by flame atomic absorption spectrometry using a Hitachi Z-5000 spectrometer. To analyse soluble iron, samples were collected, filtered, and acidified with nitric acid (HNO_3) to ensure a pH < 2. For total iron determination, the procedure was similar but the samples were not filtered. In both cases, the acidic digestion suggested in [6,27] was omitted because the samples only contained simple iron compounds, available for re-dissolution at pH < 2. This fact was experimentally confirmed.

To analyse iron by atomic absorption spectrometry in samples containing cyanide, they must be adjusted to a very low pH, which

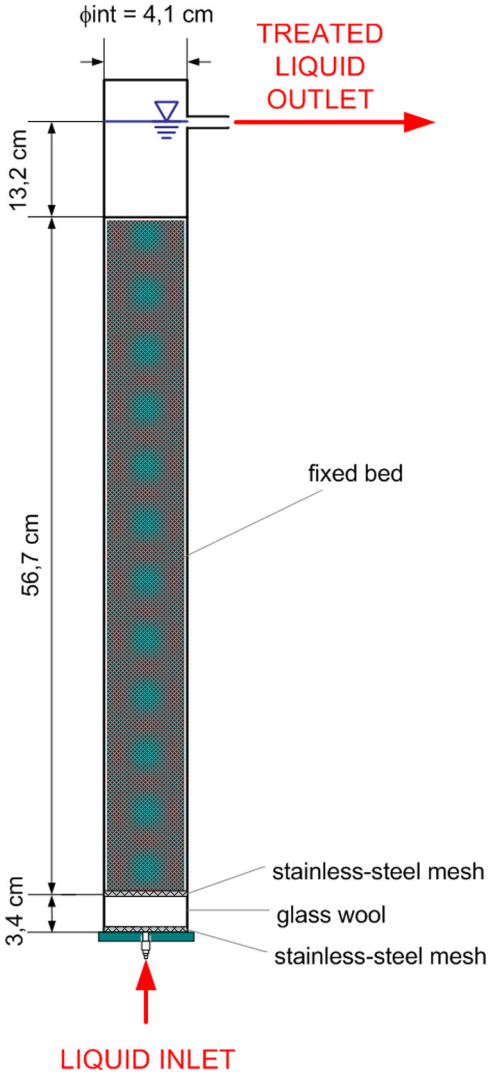

Fig. 3. Constructive detail of the fixed bed column employed in the experiments.

involves the release of dangerous hydrogen cyanide gas. In those samples, cyanide was previously removed from the samples to prevent that risk by a quantitative distillation procedure [6]. Iron was measured from the remaining solution that was obtained with the distillation used to quantify cyanide concentration. All samples were measured using the standard addition method to reduce matrix interferences. For soluble iron determinations, the samples were filtered before distillation.

Total free cyanide was measured directly in the alkaline sample using an ion selective electrode (ISE, Thermo Orion 9606BN) according to the method suggested in [6]. Soluble free cyanide was measured by the ISE method after filtration. Additional preservation was not required because the pH was >11 [6]. The lack of ISE response to complexed cyanide forms was experimentally verified [25]. Total cyanide was measured by the ISE method after the quantitative distillation procedure, already mentioned [6]. When measuring soluble cyanide, samples were filtered prior to distillation.

Fixed bed material was characterized by XRD (Shimadzu XD-D1).

Experimental procedure

The UV–ozone reactor was filled with raw liquid from a storage tank and the fixed bed was filled with reagent water. Prior to circulation through the column, the UV–ozone reactor was

operated batchwise for 120 min in order to maintain the same experimental conditions as those presented in a previous work [5]. After that, the liquid started to flow continuously through the entire system. The authors assumed steady state condition for each experiment when the outlet concentration of all measured parameters reaches a constant value and does not further changes.

Results and discussion

XRD analysis (not shown) identified the used zeolite as clinoptilolite type (66% Al, 13% Si) with a degree of crystallinity higher than 80%. The manganese that remained in the zeolite as different oxides (mainly Mn_2O_3) imparted a brown colour to the material.

Fluid-dynamic behaviour of the liquid phase

In order to identify variations in output concentration either due to chemical reactions or generated only by fluid-dynamic effects, the hydraulic behaviour of reactors was characterized.

The residence time distribution (RTD) of each reactor was studied by means of stimulus–response assays [28] using methyl orange as the inert tracer [25]. The UV–ozone reactor behaviour fitted the ideal continuous stirred tank reactor theoretical model [25,29]. Fixed bed column flow does not respond to any ideal flow model. The mathematical model representing the RTD in the fixed bed column developed in previous works [25,29], successfully fitted the experimental data obtained with stimulus–response assays in the column. The response to a unit concentration step injected into the fixed bed column is represented in the Fig. 4.

(a) Experiments with soluble iron(II)

The main time-dependent stage of this process was iron retention in the fixed bed column. Consequently, several experiments were conducted using iron(II) solutions without cyanide in order to determine the optimal hydraulic residence time and ensure acceptable iron removal levels. Operation with non-cyanide solutions during initial experiments also reduces occupational risks and hazardous waste generation. The solutions were processed in the UV–ozone reactor to maintain the same experimental conditions as those present when the removal of cyanide complexes was assayed.

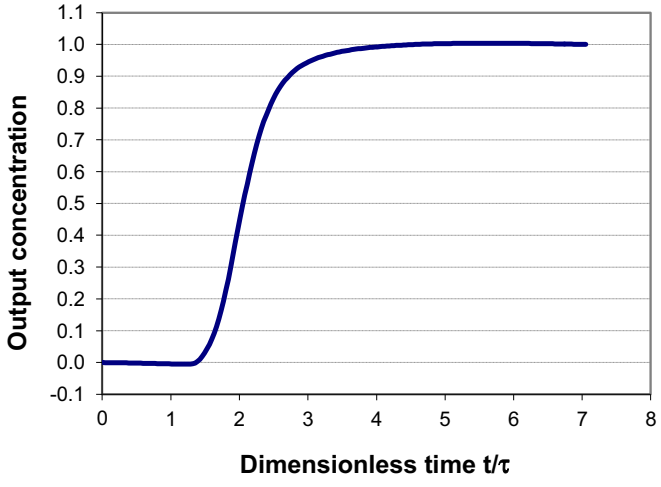

t: Time;
τ: Hydraulic Residence Time (liquid volume in the column / flow)

Fig. 4. RTD model response to a unit concentration step injected into the fixed bed column.

The experiments were carried out with three different τ values in the fixed bed column (τ = fixed bed volume × porosity/flow) in order to explore the fixed bed column behaviour. Experiments show that iron was retained reducing the concentration of total iron as liquid passed through a fixed bed column. At the column discharge, iron was found in two different forms: soluble and precipitated (as suspended solids), which corresponds to partial precipitation.

Significant iron concentration variations were observed at the column discharge (Fig. 5).

For the highest flow rate assayed (τ = 1.2 min), total and soluble iron concentration values were similar. For higher τ values, the marked difference observed between total and soluble iron concentrations indicates the presence of precipitated iron at the column discharge. Those results show that iron precipitation requires higher τ values, which suggests that the mechanisms involved have slow kinetics. As iron(III) is less soluble than iron(II) [26], the behaviour observed agree with an oxidation–precipitation mechanism. Once the solution containing iron(II) pass throughout UV–ozone reactor, it was probably oxidized to iron (III) starting the nucleation and growth of $Fe(OH)_3$ crystals. The residence time in the fixed bed column it was not enough for the crystal growth until the size required for the retention in the zeolite bed by a filtration mechanism. Then, the iron left fixed bed partially precipitated as suspended iron. The amount of precipitated iron at the column outlet changes for different τ values because there are changes in the time available for nucleation and precipitation phenomenon.

For τ = 5.0 min, a [$Fe_{soluble}$] peak is observed at 15 min (Fig. 5) while the concentration decreases below 0.028 mg/l after 45 min. For τ = 13.3 min, steady state values of [$Fe_{soluble}$] were slightly higher. Those peaks are the result of the interaction of nucleation–precipitation phenomenon (increased for higher τ) and the fluid-dynamic behaviour of the system. A τ value of 5.0 min was selected for the assays described below.

Although total iron concentration profiles show different slopes for each τ, they all reached similar steady state values after longer operating times. The total iron removal, neither was modified when the amount of precipitated iron increased, as observed for higher τ values (Fig. 5). This behaviour shows that total iron removal was not the result of precipitation–filtration phenomena but that iron was partially retained in the column by a mechanism affecting soluble forms.

Discharged liquid pH was similar to the pH at the column inlet, discarding the possibility that precipitation was only due to a modification of this parameter. Dissolved iron is present in anionic forms $[Fe(OH)_3]^-$ or $[Fe(OH)_4]^-$ at the pH used in the experiments [26]. Therefore, both total and soluble iron removal mechanisms must have affected those anionic forms.

Even the total iron removal was not dependent of UV–ozone pretreatment stage, the iron precipitation was clearly accelerated when UV–ozone pretreatment was applied (Fig. 6).

The amount of iron retained in the fixed bed was not modified by UV–ozone pretreatment, suggesting that total iron removal corresponds to a mechanism independent of the changes introduced by UV–ozone in the system. An ion-exchange mechanism in the fixed bed would fit the above observations. The UV–ozone pretreatment was found to accelerate the iron precipitation kinetics (Fig. 6). With regard to the behaviour of soluble iron, results obtained with UV–ozone pretreatment were different from those obtained when iron solution was directly fed into the column. This fact may be explained by an enhanced oxidation of iron induced by UV–ozone system. When solution with iron(II) was feed directly to the fixed bed column, a slower oxidation should

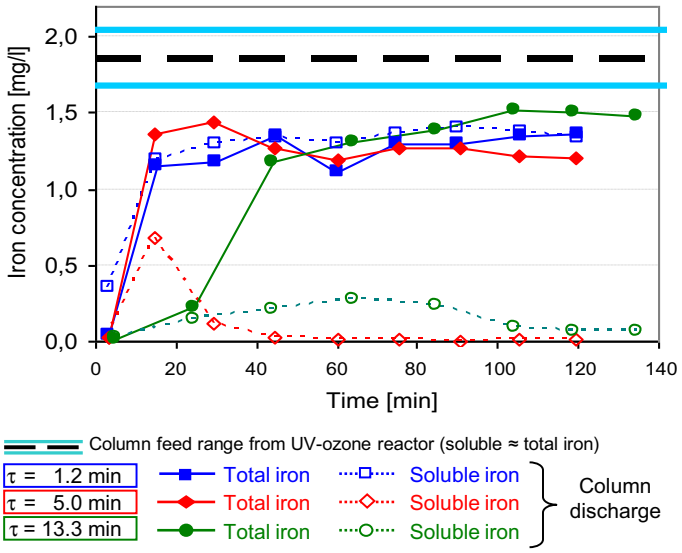

Fig. 5. Total and soluble iron concentration at the fixed bed column discharge as a function of reaction time in experiments without cyanide for different hydraulic residence times (τ) values (pH = 12.7 ± 0.1; $[Fe]_0$ = 1.9 mg/l).

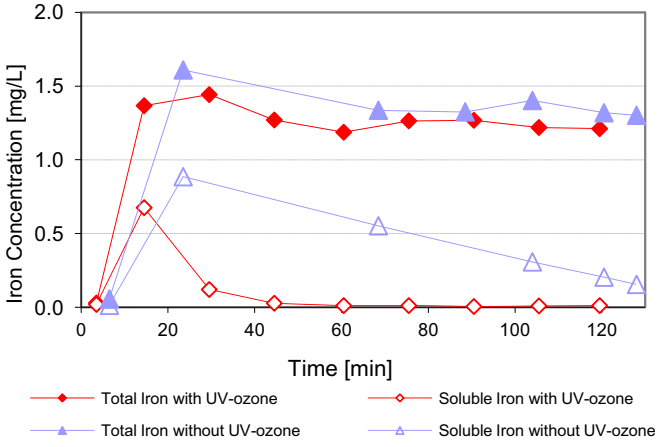

Fig. 6. Influence of the UV–ozone pretreatment on the iron concentration observed at the fixed bed column discharge as a function of the reaction time in the experiments without cyanide ($\tau_{fixed\ bed}$ = 5.0 min; pH = 12.7 ± 0.1; $[Fe]_0$ = 1.9 mg/l).

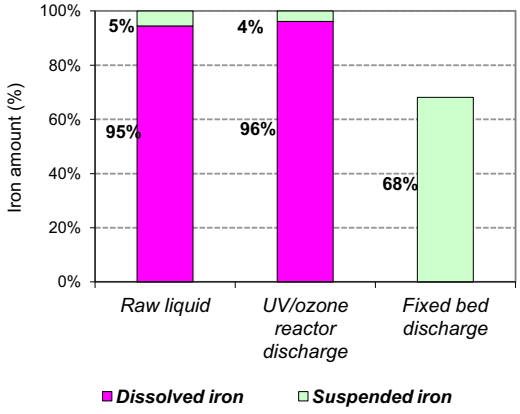

Fig. 7. Dissolved and suspended iron concentrations throughout the system in experiments without cyanide ($\tau_{fixed\ bed}$ = 5.0 min; pH = 12.7 ± 0.1; $[Fe]_0$ = 1.9 mg/l). Average values once reached the steady state condition.

have place due the effect of the oxygen present in the air, causing the nucleation and precipitation of $Fe(OH)_3$ observed.

The iron precipitation mechanism induced by the fixed bed must be examined in greater detail by further experiments. Average concentrations measured at steady state condition were used to represent the evolution of the main parameters along the system (Fig. 7).

(b) Experiments with iron cyanide complex solutions

For these experiments, the system was operated using the optimum hydraulic residence time determined through iron removal experiments (a) at a flow rate of 58 ml/min.

Free cyanide was not detected in any sample indicating that all the cyanide was complexed. The small differences between total and dissolved cyanide were attributed to analytical uncertainty, iron and cyanide were found to be completely dissolved and complexed in the raw liquid.

The UV–ozone discharge was analysed once the system had reached a steady state condition. As batch pretreatment with UV–ozone was applied for 120 min before to start the operation of the fixed bed and the residence time in the reactor was only 75 min when the system was operated continuously, the steady state condition in the reactor was considered to be representative of the entire experiment. In the UV–ozone reactor discharge, cyanide concentration was clearly lower than in the raw liquid, an indication that removal occurred in the reactor. Total iron concentration maintained the same values as at the inlet; however, 46% of this amount was found to be precipitated in the UV–ozone discharge. Therefore, cyanide removal and iron precipitation phenomena occurred simultaneously in the UV–ozone reactor.

The concentrations observed at the column discharge were time dependent, with a tendency to reach steady values over longer periods of operation. Iron and cyanide concentration profiles were delayed in time when compared to the RTD numerical model and to the results of iron removal experiments (Fig. 8). This observation may evidence a sorption–desorption phenomenon that momentarily retains the complex molecules in the bed.

Average concentrations measured at steady state condition were used to represent the evolution of the main parameters along the system (Fig. 9 and Fig. 10).

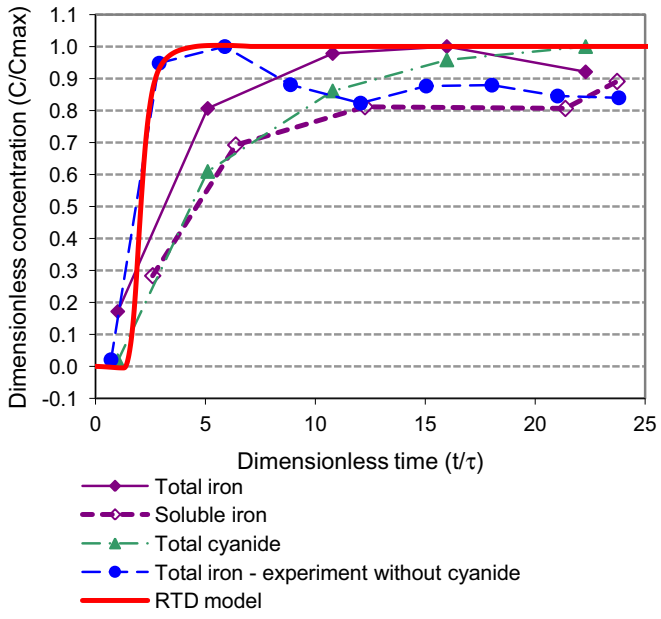

Fig. 8. Dimensionless iron and cyanide concentrations profiles discharged from the fixed bed column as a function of the reaction time. Experiments with iron–cyanide ($\tau_{fixed\ bed}$ = 5.1 min; pH = 13.5 ± 0.1; $[Fe]_0$ = 1.9 mg/l; $[CN^-]_0$ = 4.7 mg/l) compared with experiments without cyanide.($\tau_{fixed\ bed}$ = 5.0 min; pH = 12.7 ± 0.1; $[Fe]_0$ = 1.9 mg/l) and with RTD numerical model.

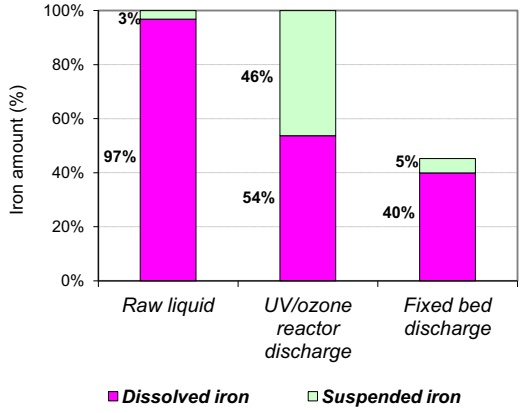

Fig. 9. Dissolved and suspended iron concentrations throughout the system in an iron–cyanide experiment ($\tau_{fixed\ bed}$ = 5.1 min; pH = 13.5 ± 0.1; $[Fe]_0$ = 1.9 mg/l; $[CN^-]_0$ = 4.7 mg/l). Average values once reached the steady state.

Total iron concentration at the column discharge was almost half (45%) of the total iron amount at the column inlet (Fig. 9). Consequently, 55% of the iron fed was retained in the column. The fraction of retained iron includes the iron previously precipitated with UV–ozone pretreatment (46%) plus an additional 9%. The iron present at the column discharge was mainly dissolved, but a small fraction was found to be present as suspended solids. The fixed bed stage did not substantially modify the concentration of cyanide in the liquid.

Most cyanide removal (66%) occurred in the UV–ozone reactor (Fig. 10). A little additional cyanide removal closer to quantification limits took place in the fixed bed totalling a 68%.

Soluble iron–cyanide molar ratios obtained from measured values were 5.4 in the raw liquid, 3.2 at the UV–ozone discharge and 4.1 at the final discharge. Therefore, the amount of cyanide ligands per iron molecule decreased throughout the process.

General discussion

The capability of ozone to oxidize free cyanide in aqueous solutions may produce CNO^-, HCO_3^-, CO_2, N_2, NO_2^- and/or NO_3^- as it was verified and reported by other authors [9,23,30,31]. Under UV radiation, the cyanide ligand of iron–cyanide complexes may be replaced by another ligand L (for example H_2O or OH^-) through a ligand substitution mechanism [4,5,10,24] (Eq. (1)).

$$[Fe(CN)_6]^{-m} + nL^k \rightarrow [Fe(CN)_{6-n}L_n]^{nk+n-m} + nCN^- \quad (1)$$

The photo-substitution reaction may progress by releasing some or even all of the cyanide ligands. Some authors [10,11] noted that ligand substitution (Eq. (1)) may compete with the iron(II) oxidation reaction producing $[Fe(CN)_6]^{3-}$. There is significant oxidation reaction in the presence of relevant amounts of certain compounds (NO_3^-, N_2O, H_3O^+). Ohno [10] and Shirom and Stein [11] attributed this observation to the electron scavenging properties of such substances.

As in the present experiments neither NO_3^- nor N_2O were present and the solution pH was alkaline, the dominant mechanism is thought to be ligand substitution. Even if NO_3^- were produced by CN^- oxidation, its concentration should be lower than the values reported by Ohno to shift the reaction to an iron oxidation mechanism.

The hypothesis of cyanide ions released from the coordination sphere followed by oxidation of those ions strongly agrees with the behaviour of iron and cyanide concentrations when the liquid circulated through the UV–ozone reactor (Fig. 9 and Fig. 10). This mechanism caused a 66% reduction in cyanide concentration (Fig. 10). As no free cyanide was detected, it is reasonable to assume that the released cyanide was immediately oxidized by $O_3/OH^\bullet$. The 46% iron precipitation (Fig. 9) corresponds to oxides or hydroxides formed from released iron after the six cyanide ligands were replaced by H_2O/OH^- molecules (Eq. (1) with $n = 6$). This hypothesis was confirmed by the absence of cyanide in the suspended solids. The dissolved CN^-/Fe molar ratio reduction observed in the reactor discharge indicates the presence of soluble complexes in which the number of iron-bonded cyanide ions is lower than six. The remaining positions in the coordination sphere were probably occupied by H_2O or OH^- groups.

Total iron concentration at the column discharge was only 45% of the fed values and it was mostly dissolved. The fixed bed column retained iron previously precipitated in the UV–ozone stage, plus an additional 9%. Only 5% of the iron fed left the column as precipitate forms. Iron oxide/hydroxide crystals precipitated in the UV–ozone reactor may grow as they pass through the column reaching sizes large enough to be removed by physical filtration in the fixed bed. Consequently, only 45% of the iron fed left the column.

Additional amounts of iron retained in the column (9%) and precipitated at the column discharge (5%) were small and may be attributed to experimental uncertainties. However, both observations must be considered as indicators of the other mechanisms that occurred in the column. These mechanisms may include either an ion exchange process, as proposed for iron removal experiments, or one of the following: crystal nucleation and growth initiated in the UV–ozone reactor, iron precipitation promoted by manganese oxides adsorbed in zeolite [5,25], and/or some kind of surface phenomenon capable of continuing the dissociation of complexes initiated in the UV–ozone reactor. The last mechanism followed by oxidation of free cyanide by residual ozone and Mn oxides may correspond to the small reduction in cyanide concentration observed in the column (Fig. 10). Some of those

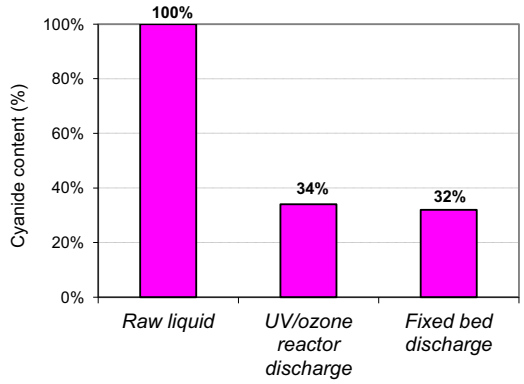

Fig. 10. Cyanide concentration throughout the system in an iron–cyanide experiment ($\tau_{\text{fixed bed}}$ = 5.1 min; pH = 13.5 ± 0.1; $[Fe]_0$ = 1.9 mg/l; $[CN^-]_0$ = 4.7 mg/l). Average values once reached the steady state.

mechanisms may occur simultaneously in the fixed bed, though this possibility needs further investigation.

Effects of cyanide on iron behaviour

Considering the iron removal experiments, no precipitated iron was found at the UV–ozone reactor discharge (Fig. 7). In these experiments, the UV–ozone reactor only enhanced the subsequent precipitation kinetics in the fixed bed stage (Fig. 6). However, in the presence of cyanide, iron was partially precipitated at the UV–ozone reactor discharge (Fig. 9) which may be due to some nucleation phenomenon that started in the UV–ozone reactor simultaneously with iron separation from cyanide complexes.

In experiments with uncomplexed iron, about 32% of the iron fed was retained in the fixed bed (Fig. 6). In this case, the nucleation phenomenon probably began in the fixed bed stage and growth time was not enough for crystals to reach a size suitable to be totally retained by filtration in the zeolite bed.

In samples containing iron–cyanide complexes (Fig. 9), the iron fraction retained in the fixed bed was higher (55%). However, 40% of the iron fed left the column in soluble forms while only a small fraction (5%) was discharged from the column as suspended solids. In the liquid discharged from the fixed bed, the close values of dissolved and total iron concentrations through time (Fig. 8) indicate a lower precipitation efficiency than the one observed in iron removal experiments with the same τ (5 min) (Fig. 5). This observation corresponds to the presence of highly soluble iron–cyanide complexes that prevent the precipitation of iron hydroxides.

Conclusions

In this paper we described a UV–ozone reactor with a fixed bed made of treated natural zeolite capable of removing iron-complexed cyanide from synthetic wastewater.

Iron was partially retained and precipitated in the fixed bed when the system processed iron solutions, without cyanide. The effect of the hydraulic residence time was studied and the optimum value for iron precipitation was adjusted. Although UV–ozone pretreatment did not remove the iron, it accelerated the precipitation of iron in the fixed bed.

Operating the system fed with a synthetic potassium hexacyanoferrate(II) solution, it removed 68% of the initial concentration of cyanide, 55% of the initial concentration of total iron and 60% of the initial concentration of soluble iron. The UV–ozone reactor is capable of removing most of the cyanide (66%) and of precipitating a significant amount of iron (46%). Iron removal mostly occurs in the fixed bed.

A delay was detected when the discharged concentration evolutions were compared with a numerical model representing the hydraulic behaviour of the liquid in the system. This may have been due to molecular interactions with the fixed bed.

It can be concluded that it is possible to improve the feasibility of application of this technology in small industries by replacing synthetic zeolite with a cheaper natural material and by developing a tandem reaction system capable of dissociating and oxidizing the complexed cyanide in a single reactor.

Acknowledgements

The authors wish to thank CTUA/INA for providing all the facilities and support for this research. They would also like to express their gratitude to H. Wada and Y. Hirayama from Nihon Wacon and the Japanese International Cooperation Agency (JICA), respectively, for the initiative, ideas and collaboration during the first stages of this research; to JICA for the acquisition of the necessary equipment; to P. Braunfeld and M. Pikeris from Centro de Economía, Legislación y Administración del Agua (CELA)/INA for the writing and language revision; to M.F. Lopolito for her participation in the project design and first experimental stages; to E. Miró, V. Milt, M.A. Ulla and N. Dreiling from the Universidad Nacional del Litoral (UNL) for analyses of fixed bed material; and to A. Zanini from FI-UBA for his collaboration in the RTD numerical modelling.

References

[1] D. Dzombak, R. Ghosh, G. Wong-Chong, Cyanide in Water and Soil – Chemistry, Risk and Management, CRC Press, Taylor & Francis Group, Boca Raton, 2006.
[2] R.R. Dash, A. Gaur, C. Balomajumder, Cyanide in industrial wastewaters and its removal: a review on biotreatment, J. Hazard. Mater. 163 (1) (2009) 1–11, doi: http://dx.doi.org/10.1016/j.jhazmat.2008.06.051. 18657360.
[3] USEPA, Capsule report: managing cyanide in metal finishing. office of research and development, National Risk Management Research Laboratory, Technology Transfer and Support Division EPA, 2000.
[4] R. Van Grieken, J. Aguado, M.J. Lopez-Muñoz, J. Marugán, Photocatalytic degradation of iron–cyanocomplexes by TiO2 based catalysts, Appl. Catal. B Environ. 55 (3) (2005) 201–211, doi:http://dx.doi.org/10.1016/j.apcatb.2004.08.008.
[5] H. Wada, K. Yanaga, Y. Kuroda, S. Hanela, Y. Hirayama, Recycling of wastewater containing iron-complex cyanides using UV photodecomposition and UV ozone oxidation in combination with an ion-exchange resin method, Bull. Chem. Soc. Jpn. 78 (3) (2005) 512–518, doi:http://dx.doi.org/10.1246/bcsj.78.512.
[6] A. Eaton, L. Clesceri, E. Rice, A. Greenberg, Standard Methods for the Examination of Water and Wastewater, twenty-first edition, APHA, Maryland, USA, 2005.
[7] R. Ghosh, D. Dzombak, R. Luthy, D. Nakles, Subsurface fate and transport of cyanide species at a manufactured-gas plant site, water, Environ. Res. 71 (1999) 1205–1216.
[8] T. Rennert, T. Mansfeldt, Sorption and desorption of iron-cyanide complexes in deposited blast furnace sludge, Water Res. 36 (19) (2002) 4877–4883, doi: http://dx.doi.org/10.1016/S0043-1354(02)00217-8. 12448531.
[9] C.A. Young, T.S. Jordan, Cyanide remediation: current and past technologies, Proceedings of the 10th Conference on Hazardous Waste Research, May 23–24, Kansas State University, Manhattan, Kansas, 1995.
[10] S. Ohno, The photochemistry of aqueous hexacyanoferrate(II) solutions. I. Photo-aquation reaction at 3660 Å, Bull. Chem. Soc. Jpn. 40 (8) (1967) 1765–1769, doi:http://dx.doi.org/10.1246/bcsj.40.1765.
[11] M. Shirom, G. Stein, Excited state chemistry of the ferrocyanide ion in aqueous solution. I. formation of the hydrated electron, J. Chem. Phys. 55 (7) (1971) , doi:http://dx.doi.org/10.1063/1.1676587.
[12] P.A. Gallerani, J. Lord, K. Klink, D. Ferguson. Managing cyanide in metal finishing (EPA 625/R-99/009) – U.S. EPA – office of research and development, National Risk Management Research Laboratory, Technology Transfer and Support Division (2000).
[13] M. Pera-Titus, V. García-Molina, M.A. Baños, J. Giménez, S. Esplugas, Degradation of chlorophenols by means of advanced oxidation processes: a general review, Appl. Catal. B Environ. 47 (4) (2004) 219–256, doi:http://dx.doi.org/10.1016/j.apcatb.2003.09.010.
[14] M.I. Litter, N. Quici, Photochemical advanced oxidation processes for water and wastewater treatment, Recent Pat. Eng. 4 (3) (2010) 217–241, doi:http://dx.doi.org/10.2174/187221210794578574.
[15] I. Oller, S. Malato, J.A. Sánchez-Pérez, Combination of advanced oxidation processes and biological treatments for wastewater decontamination—a re-

view, Sci. Total Environ. 409 (20) (2011) 4141–4166, doi:http://dx.doi.org/10.1016/j.scitotenv.2010.08.061. 20956012.
[16] F. Hassan Hussein, Advances in treating textile effluent, in: P.J. Hauser (Ed.), Photochemical Treatments of Textile Industries Wastewater, Intech, 2011, doi:http://dx.doi.org/10.5772/1039.
[17] A.L.N. Mota, L.F. Albuquerque, L.T.C. Beltrame, O. Chiavone-Filho, A. Jr. Machulek, C.A.O. Nascimento, Advanced oxidation processes and their application in the petroleum industry: a review, Braz. J. Petrol. Gas 2 (2008) 122–142.
[18] O. Legrini, E. Oliveros, A.M. Braun, Photochemical processes for water treatment, Chem. Rev. 93 (2) (1993) 671–698, doi:http://dx.doi.org/10.1021/cr00018a003.
[19] X. Domènech, W.F. Jardim, M.I. Litter, Procesos avanzados de oxidación para la eliminación de contaminantes, CNEA-CAC-UAQ, CONICET (2001) Cap. I del texto colectivo: Eliminación de contaminantes por fotocatálisis heterogénea – M. A. Blesa – Red CYTED VIII-G.
[20] J. Aguado, R. van Grieken, M.J. López-Muñoz, J. Marugán, Removal of cyanides in wastewater by supported TiO2-based photocatalysts, Catal. Today 75 (1–4) (2002) 95–102, doi:http://dx.doi.org/10.1016/S0920-5861(02)00049-4.
[21] W.S. Rader, L. Solujic, E.B. Milosavljevic, J.L. Hendrix, J.H. Nelson, Photocatalytic detoxification of cyanide and metal cyano-species from precious-metal mill effluents, Environ. Pollut. 90 (3) (1995) 331–334, doi:http://dx.doi.org/10.1016/0269-7491(95)00020-R. 15091466.
[22] R. Mudliar, S.S. Umare, D.S. Ramteke, S.R. Wate, Energy efficient – advanced oxidation process for treatment of cyanide containing automobile industry wastewater, J. Hazard. Mater. 164 (2–3) (2009) 1474–1479, doi:http://dx.doi.org/10.1016/j.jhazmat.2008.09.118. 19022578.
[23] M.D. Gurol, W.M. Bremen, Kinetics and mechanism of ozonation of Free cyanide species in water, Environ. Sci. Technol. 19 (9) (1985) 804–809, doi:http://dx.doi.org/10.1021/es00139a006. 22196603.
[24] V. Gáspár, M.T. Beck, Kinetics of the photoaquation of Hexacyanoferrate(II) ion, Polyhedron 2 (5) (1983) 387–391, doi:http://dx.doi.org/10.1016/S0277-5387(00)83934-0.
[25] S.D. Hanela, Estudio de la tratabilidad de efluentes con complejos ferrocianurados de elevada estabilidad empleando uv-ozono, Chemical Engineering Thesis, Facultad de Ingeniería, Buenos Aires University, Argentina, 2009.
[26] M.A. Blesa, P. Morando, E. Regazzoni, Chemical Dissolution of Metal Oxides, CRC Press, 1994.
[27] USEPA, Test Methods for Evaluating Solid Wastes – SW-846 on-line, USEPA, 2009.
[28] O. Levenspiel, Chemical Reaction Engineering, second edition, John Wiley and Sons, Barcelona, 1990.
[29] S. Hanela, A. Zanini, J. Durán, Modelado Numérico Y Analítico De La Distribución De Tiempos De Residencia En Un Sistema De Reactores Uv/ozono Y Lecho Fijo, Anales de XIII Reunión de Trabajo en Procesamiento de la Información y Control (RPIC), Rosario, Argentina, 2009.
[30] F.R. Carrillo-Pedroza, F. Nava-Alonso, A. Uribe-Salas, Cyanide oxidation by ozone in cyanidation tailings: reaction kinetics, Miner. Eng. 13 (5) (2000) 541–548, doi:http://dx.doi.org/10.1016/S0892-6875(00)00034-0.
[31] M.D. Gurol, T.E. Holden, The effect of copper and iron complexation on removal of cyanide by ozone, Ind. Eng. Chem. Res. 27 (7) (1988) 1157–1162, doi:http://dx.doi.org/10.1021/ie00079a012.